

Noise and Interference Characterization for MLC Flash Memories

Jaekyun Moon, Jaehyeong No
Department of Electrical Engineering
KAIST
Daejeon, Korea

Email: jmoon@kaist.edu, eee4u@kaist.ac.kr

Sangchul Lee, Sangsik Kim, Joongseop Yang and Seung Ho Chang
Department of Flash Solution Development
Hynix Semiconductor
Icheon, Korea

Email: {sangchul.lee, sangsik1.kim, joongseob.yang, shchang}@hynix.com

Abstract—This paper provides statistical analysis on real data taken from state-of-the-art MLC NAND flash memory cells. The analysis allows separation of different sources affecting the output values of the cell. Interference due to floating gate coupling is isolated. The effect of noise and interference on the victim cell after repeated program/erase cycles as well as baking is investigated.

I. INTRODUCTION

Statistical characterization of data taken from actual flash memory cells provides valuable insights. Our earlier work showed that different sources that affect the value of the read signal can be isolated and quantified based on defining mask patterns that capture a selected number of cells with respect to the position of the victim cell [1]. Various conditional probability estimates can be used to quantify the effect of particular noise/interference sources. In this paper, we provide an overview of the statistical analysis method of [1] and present the results of the analysis on data taken from the memory cells after a number of program/erase (P/E) cycles as well as baking. Baking simulates the aging process for understanding the retention characteristics while repeated P/E cycles can shed light on endurance behavior of the memory cells. Our results show that the interference characteristics remain largely unchanged with P/E cycles and baking. The random noise contributions, however, increase with baking and P/E cycles. Accordingly, random noise appears more important than the effect of interference with aging and wear.

II. STATISTICAL DATA ANALYSIS

A. Problem Statement

We discuss how, in particular, changing the input (write) value of a certain cell would affect the output (read) value of the victim cell. This type of cell-to-cell interference arises due to floating-gate voltage coupling [2]. We also investigate how the noise variance of the victim cell gets affected by the input pattern of the local cells. We show that the impact of an arbitrarily chosen cell or group of cells on the victim cell can be quantitatively understood. We are given only a limited set of data, and the statistical analysis needs be planned carefully. Let x_{jk} and r_{jk} denote the input (write) and soft output (read)

values of the jk -th memory cell. Let \mathbf{x} represent the entire inputs values for a two-dimensional (2-D) array of cells. We can write:

$$r_{jk} = x_{jk} + n_{jk}(\mathbf{x}) + f_{jk}(\mathbf{x}) \quad (1)$$

where $n_{jk}(\mathbf{x})$ is the noise associated with the jk -th cell, possibly depending on the input values of all cells \mathbf{x} , $f_{jk}(\mathbf{x})$ represents the interference on the jk -th cell that in general depends on the input values for all cells. Given a pair of input and output values for a finite-size 2-D array of cells, we wish to characterize $n_{jk}(\mathbf{x})$ and $f_{jk}(\mathbf{x})$ conditioned on a specified set of input values on an arbitrary selection of potentially interfering cells.

Let the error signal be defined by $e_{jk} = r_{jk} - x_{jk} = n_{jk}(\mathbf{x}) + f_{jk}(\mathbf{x})$. We are interested in answering the following questions. What is the probability density function (pdf) of e_{jk} conditioned on a specified local pattern of input values? Can we separate the noise from the interference? Where are the interfering cells and can we quantify their impact on the victim cell at position (j, k) ? The random variable e_{jk} represents the combination of noise and interference that depend on the input pattern \mathbf{x} .

A typical data analysis method consists of collecting the output values r_{jk} corresponding to some fixed input value x_{jk} and a specified input value for a suspected interfering cell, say, the cell at position $(j + 1, k)$, as the pass is taken over all “victim” cell positions (j, k) . Fig. 1 shows typical histogram plots for the conditional pdfs of r_{jk} obtained using this method. The suspecting interfering cell is the one below the victim cell in this case and different conditional pdfs correspond to different input levels assumed for the interfering cell. The cells can take four different input levels in our data: the erasure (ER) level and three different program voltage levels, ranging from PV1 to PV3. The victim cell was fixed at PV2 in the figure. Notice that the conditional pdfs have different means and variances, signifying that the amount of interference varies depending on the input value for the interfering cell.

While this method predicts with reasonable accuracy the mean shift in the output value of the victim cell due to the interfering cell, it does not allow isolation of the sources for the random variations around the means. For example, the

This work was supported in part by Hynix Semiconductor.

random variations in Fig. 1 include effects of both random noise and the variation of the input values for the neighboring cells.

As will be shown below, our proposed analysis method overcomes this shortcoming, allowing identification and quantitative assessment of different sources for the random variations in the victim cell's output value. In particular, our method can isolate the amount of variation in the victim cell's output value due to the changing input value of a particular interfering cell.

B. Determining the Mask Shape

Our method is based on dividing the cells into a group of potentially interfering nearby cells and the rest of cells that are distant and thus are not likely to interfere. We first define a mask that captures the potentially interfering cells. We then attempt to average out the effect of the cells outside of this mask, so a focus can be made only on likely interfering cells. The size and the shape of the mask must be chosen judiciously. Let us call the cells captured within the mask internal cells and the ones outside the external cells. Since we are dealing with a finite set of data, if the mask size is too big, there would not be enough data samples to average out the effect of the external cells. If the mask size is too small, there would not be enough samples to reliably estimate the random distribution that arises due to internal cells. In this paper, the size of the mask is limited to cover 5~9 cells. For example, the mask may be of a 3 by 3 square pattern consisting of 8 neighboring cells surrounding a victim cell in the center.

C. Analysis

Let P denote the mask shape. We also need to define a submask P' as well as $Q = P \cap \bar{P}'$. See Table I for some example mask shapes. We shall use lower case letters p, p' and q to denote the specific combination of input values for the cells under the corresponding masks. Assuming that all signal and noise processes are stationary (i.e., statistical parameters

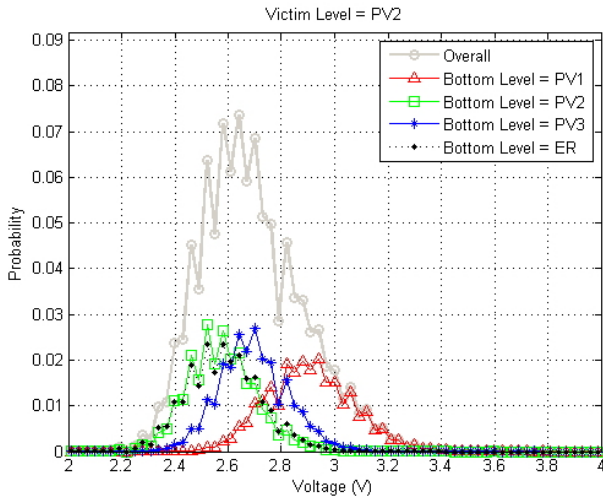


Fig. 1. Probability distributions of victim cell's output values conditioned on different input values for the interfering cell (data with no prior P/E cycles)

are position-invariant), we write the output value of the victim cell as

$$r(p) = x(p) + n(p) + f(p) + E(P) \quad (2)$$

where $x(p)$ denotes the victim cell's input value corresponding to p , a deterministic array of input values; the noise term $n(p)$ is zero-mean random variable representing the various noise sources due to random variation induced during writing and random noise during reading as well as random variations around the nominal write values in all internal cells in P ; $f(p)$ represents interference caused by the input values of the internal cells of the mask and is non-random once the internal input pattern p is fixed; and another interference term $E(P)$ denotes potential interference coming from all cells outside the chosen mask P and is a random variable if the input values of the external cells are not specified. In writing (2), we have assumed that the victim cell's noise due to random variation around the nominal write level in each external cell is negligible.

Let $r(p)$ be the collection of victim cell's output values corresponding to the specific local input pattern p . The mean of these samples is

$$\begin{aligned} \bar{r}(p) &= \bar{x}(p) + \bar{n}(p) + \bar{f}(p) + \bar{E}(P) \\ &= x(p) + f(p) + \bar{E}(P) \end{aligned} \quad (3)$$

where the over-bar denotes the mean. Assuming that the sample size is large enough, we should expect $\bar{n}(p) = 0$ for any p . Also, we have $\bar{x}(p) = x(p)$ and $\bar{f}(p) = f(p)$ since $x(p)$ and $f(p)$ are deterministic once p is given. At this point, we take a close look at the existing pdf extraction method described in II.A. We rewrite (2) with p replaced by p' to describe the victim cell's output value conditioned on a specific p' , the input values for cells under some submask P' :

$$r(p') = x(p') + n(p') + f(p') + \underbrace{E(P')}_{f(Q)+E(P)} \quad (4)$$

Notice that in (4) we are assuming $n(Q) = 0$. Now the average (taken over all possible input values for cells outside the mask

TABLE I
EXAMPLE MASK PATTERN AND SUBPATTERNS

Pattern	Definition	Example
P	A mask pattern covering the victim cell (v) and selected, potentially interfering neighboring cells (all cells shown)	
P'	A subset pattern of P including the victim cell (red+blue)	
$Q = P \cap \bar{P}'$	A pattern covering the cells in P but not those in P' (blue)	

P') is:

$$\begin{aligned}\bar{r}(p') &= \bar{x}(p') + \bar{n}(p') + \bar{f}(p') + \bar{f}(Q) + \bar{E}(P) \\ &= x(p') + f(p') + \bar{f}(Q) + \bar{E}(P).\end{aligned}\quad (5)$$

Let us compute the variance of $r(p')$:

$$\begin{aligned}\sigma_{r(p')}^2 &= E\left[\{r(p') - \bar{r}(p')\}^2\right] \\ &= \sigma_{n(p')}^2 + \sigma_{f(Q)}^2 + \sigma_{E(P)}^2\end{aligned}\quad (6)$$

where $\sigma_{f(Q)}^2$ is the victim cell's output noise contribution due to variations in the input values for the cells in Q while $\sigma_{E(P)}^2$ is due to similarly introduced interference from cells outside the mask P . It is now clear that the noise variance computed in this way is a mixture of effects from multiple sources: the pattern-dependent random noise, the input pattern variations in Q and the input pattern variations in the external cells. The existing analysis does not tell us how to separate the effects of these sources.

We now come back to our approach and show how noise sources can be isolated and analyzed. Let $\bar{r}(P)$ be the random variable representation of $\bar{r}(p)$, i.e., $\bar{r}(p)$ is a specific instance of $\bar{r}(P)$ corresponding to $P = p$. Let us fix p' and collect those $\bar{r}(P)$ values corresponding to the common p' . The histogram plot of these values reflects the distribution generated by input pattern variations for cells under Q . To see this, define the corresponding random variable as

$$\bar{r}(P|p') = x(p') + f(p') + f(Q) + \bar{E}(P) \quad (7)$$

where only $f(Q)$ is the random variable causing a distribution around some mean in the right hand side. These distributions are shown in Fig. 2. The mean of $\bar{r}(P|p')$ is

$$\bar{\bar{r}}(P|p') = x(p') + f(p') + \bar{f}(Q) + \bar{E}(P). \quad (8)$$

The variance of $\bar{r}(P|p')$ can be computed using (7) and (8) as

$$\sigma_{\bar{r}(P|p')}^2 = E\left[\{\bar{r}(P|p') - \bar{\bar{r}}(P|p')\}^2\right] = \sigma_{f(Q)}^2 \quad (9)$$

which is precisely the contribution due to the input pattern variations in Q . Thus, by carefully designing the masks P and P' (and thus Q), we are able to compute the victim's output noise variance due to the input pattern variations in specific interfering cells in Q .

Putting (6) and (9) together, we subtract out the effect of $\sigma_{f(Q)}^2$:

$$\sigma_{r(p')}^2 - \sigma_{\bar{r}(P|p')}^2 = \sigma_{n(p')}^2 + \sigma_{E(P)}^2 \quad (10)$$

the left hand side of which can be measured from the data. If $\sigma_{E(P)}^2 \approx 0$, then (10) simply quantifies the variance $\sigma_{n(p')}^2$ due to the pattern-dependent random noise.

We can also obtain $\sigma_{n(p')}^2$ in an alternative way. First write

$$r(p) - \bar{r}(p) = n(p) + [E(P) - \bar{E}(P)] \quad (11)$$

which represents mean-shifted output conditioned on a specific p . Ignoring the effect of the external cells, this simply represents the noise process that depends on the local pattern p . Let the corresponding zero-mean pdf be $z(n|p)$. The variance

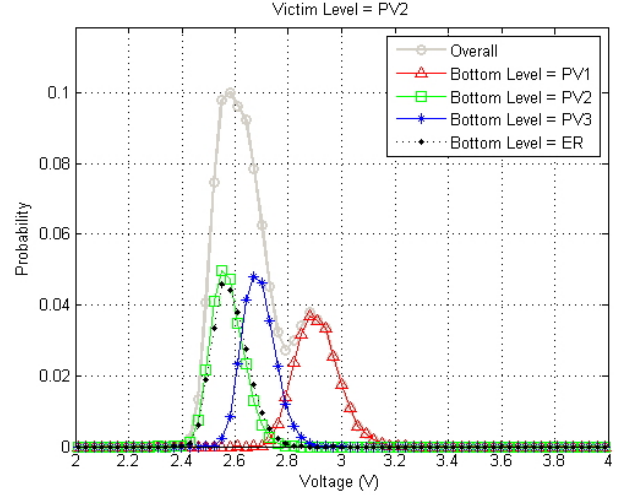


Fig. 2. Distribution of mean values $\bar{r}(P|p')$ (data with no prior P/E cycles)

associated with this pdf is $\sigma_{n(p')}^2$. Let us try to extract $z(n|p')$, whose variance is $\sigma_{n(p')}^2$. Clearly,

$$z(n|p') = \sum_q z(n|p', q) Pr(q) = \sum_q z(n|p). \quad (12)$$

which describes how $z(n|p')$ is extracted from $z(n|p)$'s. Equations (6) and (9) along with the approximation $\sigma_{E(P)}^2 \approx 0$ suggest that the convolution of $z(n|p')$ with the pdf for $\bar{r}(P|p')$ would match the pdf for $r(p')$, which is indeed the case as shown in [1]. If there is one dominant interfering cell and it is captured within the submask P' , then we would expect $\sigma_{n(p)}^2 \approx \sigma_{n(p')}^2$.

III. NUMERICAL RESULTS AND INTERPRETATION

Although not elaborated further in this paper, our data analysis indicates that the assumptions $\sigma_{E(P)}^2 \approx 0$ and $\sigma_{n(p)}^2 \approx \sigma_{n(p')}^2$ are valid and that the cell right below the victim cell has a dominating effect as far as the interference is concerned. In the sequel, we only present the data focusing on the interference effect of the bottom cell. As such the submask p' contains only the victim cell and the cell below it.

A. Pattern-dependent interference effect

Table II shows mean values of the victim cell for different combinations of the input values for the victim cell as well as the interfering cell, which in this case is the cell right below the victim cell. Five different types of data represent those from cells with no prior P/E cycles, 1.5K P/E cycles, 1.5K P/E cycles plus baking, 3K P/E cycles and 3K P/E cycles plus baking, respectively. Baking simulates one-year aging.

In all cases, the mean shift (to the right) is most pronounced when the interfering cell's input level is PV1. This is due to the fact that the change in the applied charge level is the largest when the written cell level transitions from ER to PV1, inducing the worst program disturbance effect in the victim cell. The second biggest transition is made when the target

TABLE II
MEAN : $\bar{r}(P|p')$

Victim	Bottom	P/E 0	1.5K	+bake	3K	+bake
PV1	PV1	1.35	1.36	0.96	1.39	0.78
	PV2	0.99	1.06	0.65	1.11	0.48
	PV3	1.11	1.19	0.77	1.27	0.61
	ER	1.03	1.07	0.67	1.11	0.50
	Overall	1.12	1.17	0.76	1.22	0.59
PV2	PV1	2.92	2.86	2.45	2.87	2.27
	PV2	2.59	2.59	2.19	2.63	2.03
	PV3	2.70	2.71	2.30	2.77	2.15
	ER	2.60	2.58	2.18	2.61	2.01
	Overall	2.70	2.69	2.28	2.72	2.12
PV3	PV1	4.63	4.54	4.04	4.54	3.85
	PV2	4.25	4.25	3.77	4.27	3.61
	PV3	4.37	4.37	3.88	4.40	3.72
	ER	4.29	4.26	3.78	4.28	3.60
	Overall	4.39	4.35	3.87	4.38	3.70

write level is PV3, as reflected in the second largest bias when the interfering cell's write level is PV3. We note that for the MLC cells under investigation, the two bits written into each cell originate from two separate logical pages. The first bit is written by either retaining the original ER level of the cell or programming the cell value to a level somewhat below PV2. At the writing of the second bit, if the first bit corresponded to the ER level, either the same level is retained or the charge level is raised to PV1, depending on the second bit value. If the first bit was written as the level somewhat below PV2, then the second bit would drive the new charge level to either PV2 or PV3. Raising the charge level at each programming time involves the well-known incremental step pulse programming (ISPP) method based on repeated program-verify steps with incremental increase in the programming voltage level [3]. ISPP is used to prevent cells being programmed to a charge level higher than intended, in which case the entire block must be erased again. In ISPP, the random variation around the nominal written value depends on the incremental step size [4].

As seen most clearly in the case where the interfering cell's effect is averaged (as captured in the "overall" rows), the effect of interfering cells does not change much with P/E cycles or baking. Table III shows victim cell's output variances due to input pattern variations in Q . Again, it appears that for each input value of the victim cell, $\sigma_{f(Q)}^2$ changes little across different cell types.

TABLE III
VARIANCE : $\sigma_{\bar{r}(P|p'=v)}^2 = \sigma_{f(Q)}^2$

Victim	P/E 0	1.5K	+bake	3K	+bake
PV1	0.0220	0.0185	0.0203	0.0190	0.0209
PV2	0.0226	0.0168	0.0179	0.0162	0.0187
PV3	0.0348	0.0246	0.0237	0.0223	0.0226

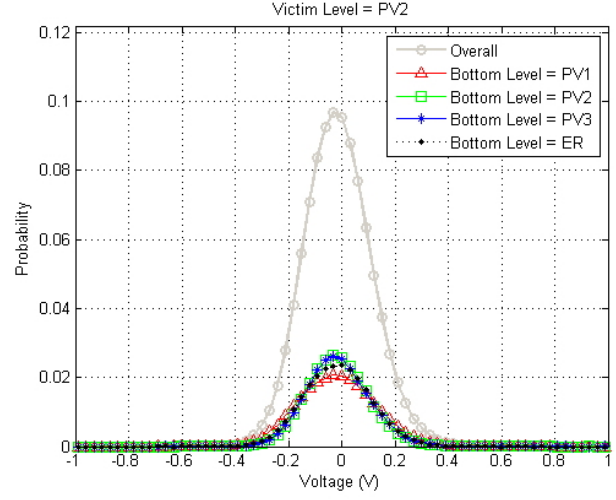


Fig. 3. Distribution of mean-shifted $r(p)$ (data with no prior P/E cycles)

B. Pattern-dependent noise variance

Table IV shows pattern-dependent noise variance for different combinations of the input values for the victim cell and the interfering cell. The pattern-dependent nature of noise is clearly revealed. In all cell types, the noise variance is the largest when the victim cell's input is PV3 and the bottom cell's input is PV1. For a given victim cell level, the noise is the largest when the interfering cell has PV1 as input. It is also clear that the noise variance increases significantly with P/E cycles and aging.

IV. CONCLUSION

Using the statistical data analysis method based on conditional means with controlled local input patterns, we are able to isolate the random noise from the effect of interference from coupled cells. Both interference and noise are clearly pattern-

TABLE IV
NOISE VARIANCE : $\sigma_{n(p')}^2$

Victim	Bottom	P/E 0	1.5K	+bake	3K	+bake
PV1	PV1	0.0173	0.0270	0.0423	0.0397	0.0616
	PV2	0.0100	0.0191	0.0322	0.0371	0.0470
	PV3	0.0105	0.0223	0.0346	0.0479	0.0515
	ER	0.0127	0.0192	0.0357	0.0330	0.0494
	Overall	0.0126	0.0219	0.0362	0.0394	0.0524
PV2	PV1	0.0203	0.0291	0.0450	0.0383	0.0635
	PV2	0.0138	0.0202	0.0374	0.0310	0.0546
	PV3	0.0145	0.0221	0.0382	0.0367	0.0560
	ER	0.0156	0.0219	0.0399	0.0307	0.0578
	Overall	0.0160	0.0233	0.0401	0.0342	0.0580
PV3	PV1	0.0459	0.0574	0.0743	0.0664	0.0920
	PV2	0.0364	0.0439	0.0625	0.0532	0.0784
	PV3	0.0367	0.0456	0.0633	0.0551	0.0791
	ER	0.0400	0.0512	0.0678	0.0596	0.0852
	Overall	0.0398	0.0495	0.0670	0.0585	0.0837

dependent. Different types of memory cells with different P/E cycles and with/without baking have also been analyzed. The effect of interference does not change much with repeated P/E cycles or aging. The noise, on the other hand, increases significantly with P/E cycles and with aging.

REFERENCES

- [1] J. Moon, J. No, S. Lee, S. Kim and J. Yang, "Statistical Analysis of Flash Memory Read Data," *IEEE GLOBECOM*, Dec. 2011.
- [2] J. Lee, S. Hur and J. Choi, "Effects of floating-gate interference on NAND flash memory cell operation," *IEEE Electron Device Letters*, vol. 23, pp. 264-266, May 2003.
- [3] K. Suh, B. Suh, Y. Lim, J. Kim, Y. Choi, Y. Koh, S. Lee, S. Kwon, B. Choi, J. Yum, J. Choi, J. Lim and H. Lim, "3.3 V 32 Mb NAND flash memory with incremental step pulse programming scheme," *IEEE Journal on Solid-State Circuits*, vol. 30, no. 11, pp. 1149-1156, Nov. 1995.
- [4] Guiqiang Dong, Shu Li and Tong Zhang, "Using Data Postcompensation and Predistortion to Tolerate Cell-to-Cell Interference in MLC NAND Flash Memory," *IEEE Trans. Circuits and Systems*, vol. 57, no. 10, pp. 2718-2728, Oct. 2010.
- [5] K. Kim, "Future memory technology: Challenges and opportunities," in *Proc. Int. Symp. VLSI Technol.*, pp. 5-9, Apr. 2008.